Dynamic spectral interferometry for measuring the nonlinear amplitude and phase response of a saturable absorber mirror

Gero Stibenz[a] and Günter Steinmeyer
Max-Born-Institut für Nichtlineare Optik und Kurzzeitspektroskopie, Max-Born-Strasse 2a, D-12489 Berlin, Germany

Wolfgang Richter
BATOP GmbH, Theodor-Körner-Strasse 4, D-99425 Weimar, Germany

(Received 13 October 2004; accepted 5 January 2005; published online 15 February 2005)

We report on spectral interferometry for measuring the spectrally resolved nonlinear phase and amplitude response in a pump–probe experiment. Using nJ pulses from a femtosecond oscillator, we demonstrate the method by measuring the nonlinear response of a GaAs/AlGaAs single-quantum-well saturable absorber mirror. The demonstrated sub-mrad phase sensitivity constitutes a two-order-of-magnitude improvement of phase resolution, compared to earlier demonstrations. Dynamic spectral interferometry proves to be a powerful tool for evaluating the phase response on nonlinear optical semiconductor devices for mode locking of lasers, optical switching, and other photonic applications. © *2005 American Institute of Physics*.
[DOI: 10.1063/1.1868861]

Saturable absorber mirrors (SAMs[1–3]) have become a key element for short pulse generation via passive mode locking of solid-state lasers in the near-infrared spectral region. These nonlinear optical switches mostly rely on the saturable absorption of single or multiple quantum wells (QWs). The optical amplitude response of such devices has been extensively studied, and femtosecond pump–probe measurements are a standard tool for characterization of SAM devices prior to their use in a laser. The nonlinear phase response of a SAM, however, is only accessible by indirect means. From the known amplitude response one can compute the corresponding phase response via a Kramers-Kronig transformation.[4] However, this transform is known to be extremely sensitive to weak absorption changes in the spectral wings of the measurement window. Moreover, it completely misses out absorption changes outside the spectral measurement window, as can be caused by nonresonant nonlinearities, e.g., by two-photon absorption. Real-world devices, such as SAMs, may exhibit additional nonlinear mechanisms. For example, Garnache *et al.* recently reported soliton-like pulse shaping mechanisms in the absence of negative dispersion and suspected Kerr-type nonlinear phase contributions from the Bragg stack of their SAM device as responsible for their findings.[5] Currently, there is a trend towards integration of multiple functionalities into single intracavity components and towards the increased use of thin-film devices as mode locker, gain medium, and for dispersion compensation.[3] In turn, more sophisticated diagnostic tools are required to investigate the interplay of linear and nonlinear mechanisms in such devices.

This calls for improved measurement techniques that allow for a sensitive determination of nonlinear phase changes in such devices. Several approaches to measure induced phase changes in a pump–probe-type experiment have been reported.[6–9] Some of these approaches[6,9] allowed for spectral resolution of the phase response, however, at the expense of a strongly reduced sensitivity, which renders them inappropriate for measuring nonlinear phase changes in thin semiconductor films.

Here we demonstrate spectral interferometry[10] for spectrally resolving the nonlinear phase response of a single QW with mrad resolution in addition to the fs time resolution of a pump–probe setup. The measurement simultaneously delivers the spectrally resolved amplitude response. We use a 10-fs-Ti:sapphire laser oscillator with nJ pulse energies. The setup shown in Fig. 1 employs reflective optics wherever possible. We also precompensated for residual dispersion to ensure a 10-fs-time resolution (not shown). A Mach-Zehnder interferometer detects pump-induced spectral phase differences in a noncollinear cross-polarized pump–probe experiment. In this setup, the probe beam acts as one interferometer arm, a reference beam in the other interferometer arm acts as a local oscillator. The resulting spectral interferogram is dispersed in a 0.5 m spectrograph and detected by a 2048 pixel line-scan camera, covering the entire wavelength range from 715 to 890 nm in a single shot. The externally triggered

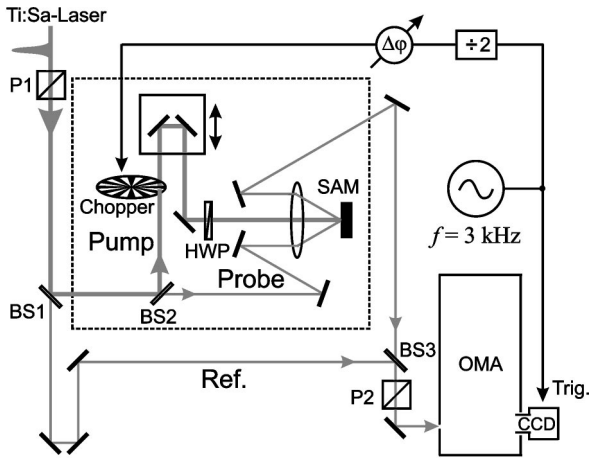

FIG. 1. Experimental arrangement for dynamic spectral interferometry. (P) polarizer; (HWP) half-wave plate; (BS) beam splitter; (SAM) saturable absorber mirror; (OMA) optical multichannel analyzer.

[a]Electronic mail: stibenz@mbi-berlin.de

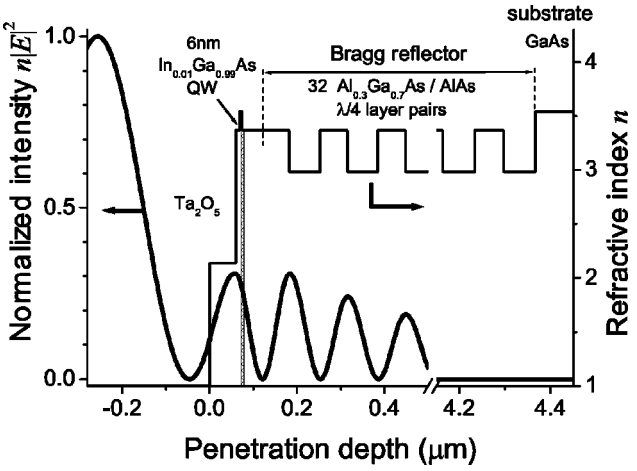

FIG. 2. Refractive index profile of the SAM (thin solid line) and electric field standing-wave pattern at 840 nm (thick solid line).

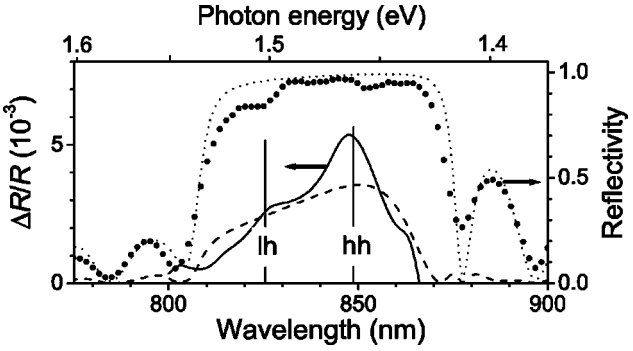

FIG. 3. Calculated (dashed) and measured (solid line) saturable reflectivity, integrated over all delays. Vertical lines indicate the first heavy hole and light hole exciton resonances apparent in the measurement. The measured (dots) and calculated (dotted line) reflectivity are shown for comparison.

CCD-camera records 3000 interferograms per second and is phase synchronized to a chopper in the pump beam running at half the trigger frequency, i.e., every other acquired interferogram is a reference measurement without the pump. The recorded interferograms are immediately Fourier transformed. One modulation side peak is isolated and transformed back into the spectral domain.[11] Absolute value and argument of the Fourier filtered data then give access to the amplitude and phase of the signal, respectively. To sensitively extract the small nonlinear response of the sample, we sum up amplitude and phase differences between odd and even numbered shots of the camera. For the experimental data discussed below, we recorded 400 000 interferograms for each time delay and repeated this procedure to cumulate 20 scans to suppress drift problems. This way we can measure extremely small phase differences on the order of 1 mrad, which corresponds to a wavelength shift of the fringe pattern in the interferograms of $\approx 5\times 10^{-4}$ nm, i.e., much less than the resolution of the spectrograph of 0.085 nm.

For a demonstration of this method, we use the SAM shown in Fig. 2. This SAM consists of a single 6 nm thick $In_{0.01}Ga_{0.99}As$ QW, embedded in an $Al_{0.3}Ga_{0.7}As$ barrier, followed by a Bragg reflector of 32 quarter wave $Al_{0.3}Ga_{0.7}As/AlAs$ pairs centered at 840 nm. The semiconductor structure is capped with a 60 nm thick Ta_2O_5 layer. A computation of the resulting intensity pattern[12] is also displayed in Fig. 2. Figure 3 shows the calculated reflectivity of the Bragg stack and an independent measurement with a spectrograph.

Using data from Refs. 13 and 14, we calculate the $n=1$ heavy hole (hh) and light hole (lh) exciton energies as 1.47 and 1.51 eV, respectively. These values agree within 5 to 10 meV with spectral response maxima of the measured signal in Fig. 3. Typical results of spectrally resolved pump–probe measurements in phase and amplitude are shown in Fig. 4. The beams are focused to a spot size of 35 μm, resulting in a pump and probe fluence of 50 and 1 $\mu J/cm^2$, respectively, i.e., well below the saturation fluence of ≈ 70 $\mu J/cm^2$. The rise time of the pump–probe traces is about 50 fs and is limited by the spectral width of the Bragg reflector rather than the 10-fs-pulse duration used.

A more detailed look at the pump–probe response for one particular delay is displayed in Fig. 5. Figure 5(a) shows the differential reflected amplitude with its excitonic substructure. The corresponding nonlinear phase changes amount to a few mrad [thick solid line in Fig. 5(b)]. We also computed the spectral phase from the amplitude data in Fig. 5(a), which is shown as a dashed line in Fig. 5(b). Thermally induced phase changes [Fig. 5(c)] were subtracted from the data in Figs. 4(a) and 5(b). These thermal phase contributions can be traced back to refractive index changes inside the Bragg mirror, causing a shift of its center wavelength by 0.04 nm.[15] From the magnitude of the observed phase changes, we deduce a temperature variation between pumped and unpumped sample of 0.2 K. Generally, the measured nonthermal phase changes [Fig. 5(b)] exhibit only small deviations from the Kramers-Kronig relation. In contrast to the findings of Ref. 5, we could not find any indications for quasi-instantaneous contributions to the nonlinear phase in our sample. At first sight the observed residual ripple on the measured phase may appear as noise or artifact. However, a closer look reveals that the zero crossings of the fine oscillations of the measured phase exactly correspond to spectral maxima of the amplitude response. Each of the exciton peaks gives rise to a positive (+) or negative (−) phase shift at wavelengths above or below the peak, respectively. We further note that these small but systematic spectral phase variations are reproduced with peak-to-peak excursions of less than 0.5 mrad. In comparison, the magnitude of the measured nonlinear phase effects reported in Ref. 9 was larger

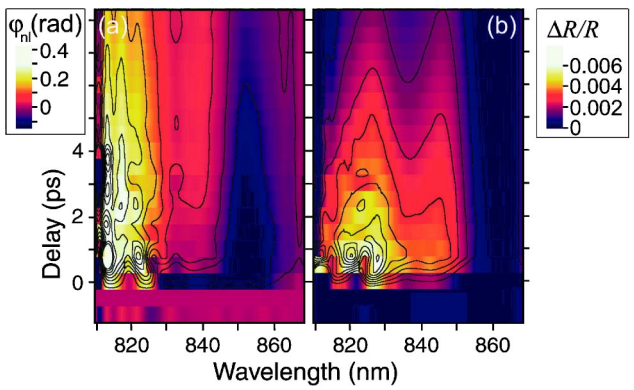

FIG. 4. (Color online) Spectrally resolved measurement of nonlinear phase (a) and amplitude (b) changes. A decay time $\tau_{1/e}=6.5$ and 12 ps is observed at the lh and hh exciton peaks, respectively. The rise time of the pump–probe traces is about 50 fs and is limited by the spectral width of the Bragg reflector, rather than the 10-fs pulse duration used.

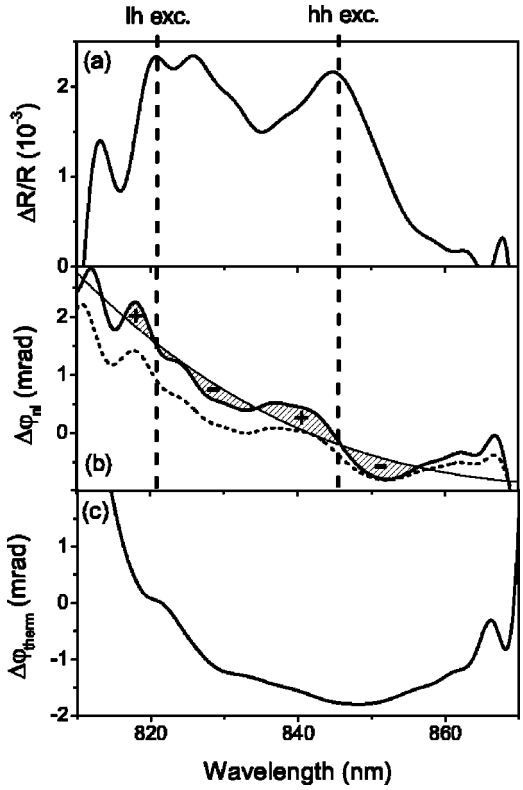

FIG. 5. Spectrally resolved pump–probe measurement: (a) Amplitude at 9 ps delay; (b) nonlinear phase change at 9 ps (thick solid line). Deviations from a polynomially smoothed phase (thin solid line) are explained by the Kramers–Kronig relation (dashed line); (c) thermal phase change at negative delays.

than 1 rad. The $\Delta n/n=10^{-5}$ sensitivity of the approach reported in Ref. 6 corresponds to a nonlinear phase change of 0.25 rad in the 1-mm-waveguide device used. Clearly, our method is at least two orders of magnitude more sensitive in terms of nonlinear phase changes and therefore much more suitable for use with thin film devices. The main sensitivity advantage comes from the detection of interferograms at kHz rates and lockin-like noise rejection after reconstructing the phase from the spectrogram. Accordingly, we found that the sensitivity roughly scales with the square root of the number of acquired interferograms. If scanning of the delay is not required, the sensitivity could easily be further enhanced to resolution of sub-100-μrad effects.

With the demonstrated phase resolution, dynamic spectral interferometry is an interesting diagnostic tool for all kinds of nonlinear switching devices. Compared to previous methods, our approach provides spectrally detailed information on the nonlinear response of the device, both in amplitude and in phase. Dynamical spectral interferometry satisfies the increased diagnostic demands for characterizing nonlinear switching elements for use in extremely compact cavities, enabling a deeper view into the complex optical processes in this emerging field.

The authors gratefully acknowledge helpful discussions with T. Elsaesser, U. Griebner, and J. W. Tomm, MBI Berlin.

[1]S. Tsuda, W. H. Knox, E. A. Desouza, J. Wy, and J. E. Cunningham, Opt. Lett. **20**, 1406 (1995).
[2]U. Keller, K. J. Weingarten, F. X. Kärtner, D. Kopf, B. Braun, I. D. Jung, R. Fluck, C. Hönninger, N. Matuschek, and J. aus der Au, IEEE J. Sel. Top. Quantum Electron. **2**, 435 (1996).
[3]U. Keller, Nature (London) **424**, 831 (2003).
[4]R. Jin, J. Okada, G. Khitrova, H. M. Gibbs, M. Pereira, S. W. Koch, and N. Peyghambarian, Appl. Phys. Lett. **61**, 1745 (1992).
[5]A. Garnache, S. Hoogland, A. C. Tropper, I. Sagnes, G. Saint-Girons, and J. S. Roberts, Appl. Phys. Lett. **80**, 3892 (2002).
[6]M. J. La Gasse, K. K. Anderson, C. A. Wang, H. A. Haus, and J. G. Fujimoto, Appl. Phys. Lett. **56**, 417 (1990).
[7]C. T. Hultgren and E. P. Ippen, Appl. Phys. Lett. **59**, 636 (1991).
[8]K. L. Hall, A. M. Darwish, E. P. Ippen, U. Koren, and G. Raybon, Appl. Phys. Lett. **62**, 1320 (1993).
[9]L. Brzozowski, E. H. Sargent, A. S. Thorpe, and M. Extavour, Appl. Phys. Lett. **82**, 4429 (2003).
[10]F. Reynaud, F. Salin, and A. Barthelemy, Opt. Lett. **14**, 275 (1989).
[11]M. Takeda, H. Ina, and S. Kobayashi, J. Opt. Soc. Am. **72**, 159 (1982).
[12]J. H. Apfel, Appl. Opt. **15**, 2339 (1976).
[13]*Handbook Series on Semiconductor Parameters*, edited by M. Levinstein, S. Rumyantsev, and M. Shur (World Scientific, London, 1996); http://www.ioffe.ru/SVA/NSM.
[14]V. Voliotis, R. Grousson, P. Lavallard, and R. Planel, Phys. Rev. B **52**, 10725 (1995).
[15]J. L. Shen, C. Y. Chang, W. C. Chou, M. C. Wu, and Y. F. Chen, Opt. Express **9**, 287 (2001).